

# Post-tensioned splice system for precast, prestressed concrete piles: Part 3, capacity verification from laboratory and full-scale testing

Zhongxin Wu, Kevin Johnson, Gray Mullins, and Rajan Sen

- Splicing precast, prestressed concrete piles has historically been difficult because the attachment detail either requires preplanned considerations and cast-in connection details or onsite coring and doweling when unplanned pile extensions are needed.
- An alternative pile-splicing approach incorporating post-tensioning was developed. The concept eliminates the limitations on tension stresses during driving.
- This is the third of three papers that detail the development and implementation of this alternative approach, and it covers the laboratory and full-scale flexural testing of spliced piles and the comparison to one-piece, unspliced piles.

**T**his is the third of three papers describing the development of a new post-tensioning system for splicing prestressed concrete piles. The first paper covered conceptual design of the proposed system and the development of its component parts.<sup>1</sup> The second paper presented findings of a side-by-side comparison of the field driving performance of a full-sized, 100 ft (30 m), post-tensioned, spliced pile with that of a similar one-piece, unspliced pile.<sup>2</sup> This paper describes how the system for fabricating laboratory and full-sized spliced specimens was implemented, as well as how testing was performed to verify bending capacity.

The transformation of a concept into a prototype inevitably requires modifications, especially during the initial stage of development. The rationale for the incremental adjustments is documented in the paper.

## Objectives and scope

Currently available pile-splicing systems for prestressed concrete piles tend to rely on principles and concepts such as welding, bolting, or doweling, which are geared more for connecting steel or reinforced concrete components. As a result, the tensile capacity of the pile in the spliced zone is small. This is reflected in specifications by limits of 500 psi (3400 kPa) on the maximum tensile stress for pile splices with mechanical connectors and 250 psi (1700 kPa) for epoxy dowel splices compared with over 1300 psi (9000 kPa) for a one-piece, unspliced pile.<sup>3</sup> Because large tensile stresses can develop in long piles driven through soft intermediate soil layers, the driving efficiency for spliced prestressed concrete piles is adversely affected. Thicker pile cushions, frequent cushion replacements, and lower hammer fuel settings are all consequences of pile splices that collectively reduce installation speed.

This research project aimed to eliminate the shortcomings of current pile-splicing methods through the development of a new post-tensioning system. A key element of the design is the use of dual embedded anchorages. This ensures that the precompression is confined only to the spliced region. The practicality of the new system has been demonstrated by the ease of its fabrication in commercial prestressing facilities.<sup>2</sup>

This paper details implementation of the new post-tensioning splicing concept in which laboratory and full-sized specimens were fabricated, spliced, and tested to failure. In both cases, the post-tensioning splicing operation and grouting were conducted in a laboratory setting. In the final phase, fabrication, splicing, and grouting were all conducted at different commercial facilities located close to the site used for pile driving.<sup>2</sup> Complete details of all three phases of this research may be found in the final report.<sup>4</sup>

## Design and fabrication of spliced specimens

All spliced specimens were cast as two half-pile segments so the splice was located at the middle, where bending moments are highest under four-point bending. This was the test setup used previously by the Florida Department of Transportation (FDOT) to assess the efficiency of other spliced pile technologies.<sup>5,6</sup>

Three sets of splice specimens were fabricated. Adjustments were made to the original conceptual framework after each set to simplify fabrication and improve system performance based on the accumulated experience. A one-piece pile was cast along with each spliced pile specimen to serve as a comparison control.

Ten pile specimens were cast altogether: four 10 ft (3 m) long, 14 in. (360 mm) piles; two 20 ft (6 m) long, 14 in. piles; two 20 ft long, 24 in. (610 mm) piles; and two 40 ft (12 m) long, 24 in. piles. The 14 in. specimens were cast in laboratory con-

ditions and are referred to as “laboratory specimens.” The 24 in. specimens were cast at a commercial prestressing facility and are referred to as “full-scale specimens.”

The strand configurations for the pile specimens were based on FDOT standard specifications.<sup>7</sup> The post-tensioning was accommodated by placing splicing ducts and strands between the prestressing strands (**Fig. 1**).

The post-tensioning ducts were symmetrically positioned around the cross section and over the transfer length of the segments being spliced. They were placed in four layers in the 14 in. (360 mm) piles (highlighted in Fig. 1) and in seven layers in the 24 in. (610 mm) specimens. Over the transfer length, the placement of the anchorages for the splicing strands was staggered to provide gradual superposition of post-tensioning and pretensioning forces and would not lead to excessive precompression.<sup>1</sup>

Figure 1 shows that there are fewer splicing strands in the outer tension regions compared with the number of strands in the one-piece pile. Thus, for the 14 in. (360 mm) pile there are three strands, compared with two splicing strands. For the 24 in. (610 mm) pile, the corresponding numbers are six (one piece) and five. This indicates that the ultimate bending capacity of the spliced pile will be smaller if it uses the same size of strands as the one-piece pile.

The cracking moment depends on the effective prestress at the splice joint and the tensile strength of concrete. It is, therefore, independent of the layout of the post-tensioned splicing strands as long as the arrangement remains symmetrical. Because the epoxy used to bond the two splicing interfaces has a much higher tensile strength, cracking will be controlled by the concrete tensile strength.<sup>8</sup> As a result, cracking can be expected to be initiated in the concrete directly adjacent to the splice interface.

## First laboratory specimen

Figure 9 of Part 1 of this paper<sup>1</sup> shows the splicing components for the first 14 in. (360 mm) laboratory specimen, which include a splicing header, post-tensioning ducts, anchorage assemblies, and a jacking plate. In the casting bed, the ducts extended the full length from within the lower pile segment, through the splice header and the upper pile segment, and terminated at the top of the upper pile segment in the jacking plate cast into the pile. In the lower segment, the ducts extended past the anchorages to a common grouting manifold, which allowed grout to flow through all ducts after stressing. The first laboratory spliced pile used smooth, thin-walled metal ducts.

The 14 in. (360 mm) laboratory specimens were cast in a specially constructed self-stressing bed designed to cast two side-by-side 20 ft (6 m) pile specimens at a time. A control and two half-pile segments were cast during each concrete placement (**Fig. A1** [for appendix figures, go to [www.pci.org/Mullins\\_Appendix](http://www.pci.org/Mullins_Appendix)]). The bed was constructed from three

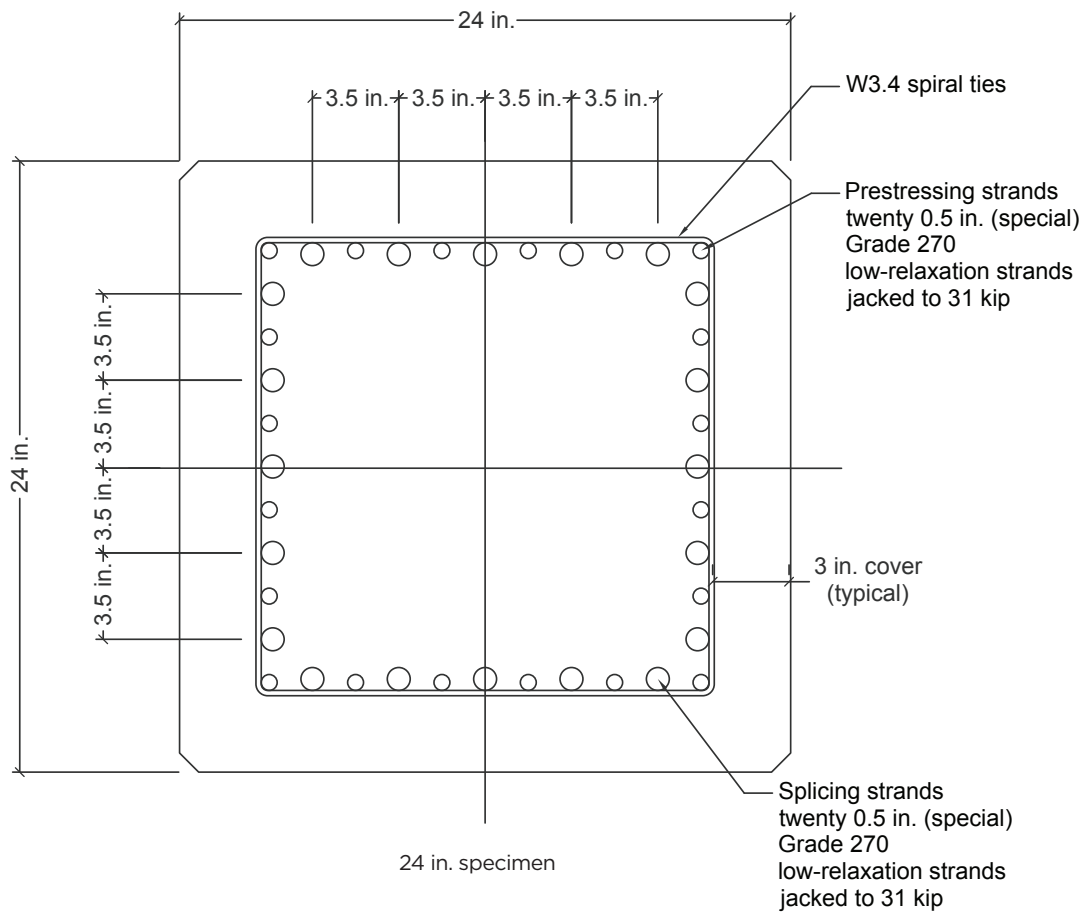
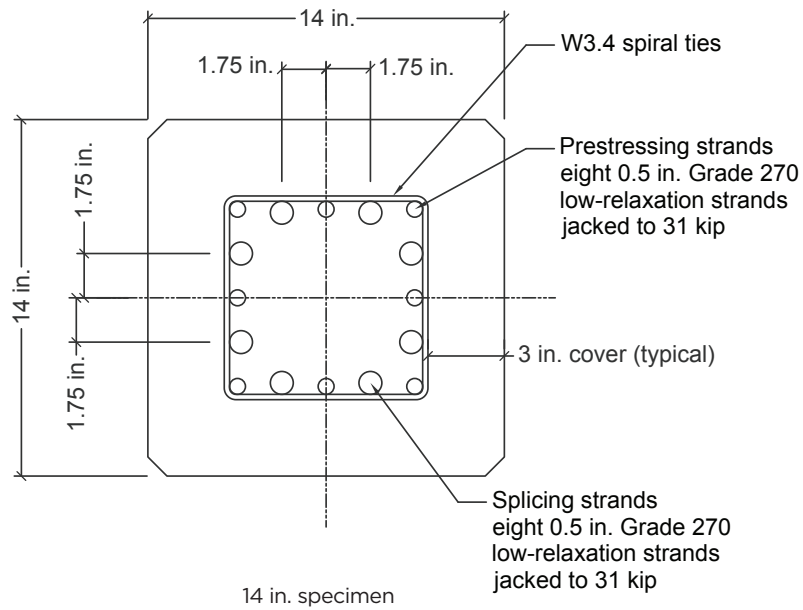


**Figure 1.** Location of post-tensioning ducts. Note: Grade 270 = 1860 MPa; 1 in. = 25.4 mm; 1 kip = 4.448 kN.

commercially cast 14 in. concrete piles. Top-face-down placement of the commercial piles conveniently provided the correct side slope while also achieving the strength to withstand the compressive loads imposed by the prestressing strands for the laboratory specimens.

Two sets of 14 in. (360 mm) spliced specimens were cast and evaluated before scaling up to the full-scale 24 in. (610 mm) specimens cast in a commercial prestressing facility.

## Layout of embedded post-tensioning anchorage assembly

The post-tensioning force was designed to be applied only to the splice zone through the use of dually embedded anchorages. This zone extended over the transfer length (50 to 160 strand diameters) of each of the two segments being spliced.<sup>9</sup> Additional length was provided in the lower segment beyond the embedded anchorages to provide sufficient strand length to develop ultimate capacity beyond the cracking moment, that is, at least 57 in. (1450 mm) from the splice interface.<sup>10</sup> This was not a consideration for the 10 ft (3 m) long upper segment.

The locations of the embedded anchorages were staggered to allow gradual transition and superimposition of post-tensioning stresses with the linearly increasing prestress over the transfer length.<sup>1</sup> The anchorages were positioned in pairs, 10, 20, 30, and 40 in. (250, 510, 760, and 1010 mm) from the splice interface. Because all ducts were the same length (50 in. [1270 mm]), the corresponding distances in the other pile were 40, 30, 20 and 10 in., respectively. Layers 1 through 4 (Fig. 1) refer to the four levels where splice strands existed in the cross section. In layers 1 and 4, the strands were closer together. In layers 2 and 3, the strands were along the outside edges.

The duct pairs were symmetrically located about the pile centroid to minimize torsional or bending effects during post-tensioning. Steel confinement spirals attached to each anchorage (Fig. A2) were designed to increase the localized compressive strength of the concrete by 4000 psi (28 MPa) and extended 6 to 7 in. (150 to 180 mm) directly in front of the anchorage bearing plates.

## Transfer length

After concrete was placed and cured, strain gauges were attached to the upper face of the spliced pile specimen. Gauges were placed 5, 15, 25, 35, and 45 in. (130, 380, 630, 890, and 1140 mm) from each of the four ends of the two half-pile segments being spliced (20 gauges in all). At the time of detensioning, the transfer length was determined as the point where constant strain was registered. These lengths ranged from 30 to 50 times the strand diameter (15 to 30 in. [380 to 760 mm]). The transfer length at the dead and splice ends was the shortest; it was longest at the live end (location 240 in. [6100 mm]). The compressive strength of concrete at the time of transfer was 6396 psi (44.10 MPa). From the average strain of 225  $\mu\epsilon$ , the prestress at transfer was 1025 psi (7.067 MPa).

## Splicing first prototype pile

### Checks

Before the splicing operation was attempted, each duct was inspected using a borescope to check whether any foreign objects had been inadvertently introduced (Fig. A3). In cases where debris was observed, it was blown out using compressed air.

The debris appeared to be steel filings caused by cutting the ducts running through the header at the time of detensioning. In subsequent fabrication, ducts were not run through the header but were terminated at the splice interface with threaded duct ends. These ends were then bolted to the splice header, which held them in the correct position and prevented entry of liquid concrete and cuttings.

Because the splicing process required that strands be pushed through embedded chucks, the wedges must be free to fully depress. Strands that only partially passed through could become stuck before reaching full insertion. Therefore, additional checks were implemented to measure the movement of the spring-actuated wedges. A 48 in. (1220 mm) long,  $\frac{3}{4}$  in. (19 mm) diameter rod was inserted inside each duct (Fig. A4) to depress the wedges, and the spring movement was measured. Normal wedge movement for the bottom pile was  $\frac{3}{8}$  in. (9.5 mm), while upper pile wedge movement was  $\frac{1}{4}$  in. (6 mm). As discussed in part 1,<sup>1</sup> the upper pile wedges were equipped with two 0.06 in. (1.5 mm) thick movement-restricting shims, which corroborated the observed movement ( $\frac{3}{8} - 0.12 \sim \frac{1}{4}$  in.).

### Splicing steps

In preparation for splicing, eight splicing strands were cut to lengths of 19 ft (5.8 m). They extended 10 ft (3 m) through the upper segment and provided enough length (3 ft [0.9 m]) for the jacking operations at the top and 6 ft (1.8 m) for insertion into the bottom segment anchorages.

The strands were first threaded into the upper pile segment from the splice end through the one-way wedges (in the chucks) and out the top of the pile. The strands were then clamped to prevent further movement into the upper segment during splicing, when the strands would be pushed into the lower pile anchorages.

The two pile segments were aligned horizontally on a 14 in. (360 mm) wide splicing rail made of two steel angles. Starting with a separation of 6 ft (1.8 m) between the two segments, the lower segment was supported by an overhead crane while still in soft contact with the rail, and a forklift was used to push it gradually toward the upper segment as strands were fed into the lower segment (Fig. A5).

To prevent strands from simultaneously entering the lower segment ducts, all eight strands exposed at the bottom of the upper segment, were staggered in length by an additional 1 in. (25 mm). As each strand reached the respective anchorage in

the lower pile, some manipulation was required if the strand was not centered as it entered the wedges. This involved simply pulling and bending the strand laterally, which pulled the end of the strand away from the wedge face until it slipped into the wedges. In some cases, the strand was rotated to assist the centering. The anchorages closest to the pile face (for example, 10 and 20 in. [250 and 500 mm]) were engaged first while the splicing strands were still relatively flexible, but for the deeper anchors (for example, 30 and 40 in. [760 and 1020 mm]), the strand length remaining between the segments was shorter and stiffer, making manipulation more difficult. There was only a 10 in. gap between segments when the last anchorage was engaged. In subsequent operations, the length of the exposed strand was increased to retain flexibility; excess length could be pushed out of the top after the clamps were removed.

With all strands inserted and anchorages engaged, nonsag epoxy was applied to both faces before final contact (**Fig. A6**). Final adjustments were made using the overhead crane to ensure that the two pieces were correctly aligned. Pipe-type alignment pins were designed for subsequent specimens, which threaded into the duct ends. This would self-align the pile segments, provide a barrier to prevent epoxy from filling the ducts, and help ensure that grout flowed easily between segments.

## Post-tensioning the splice

The stressing order was designed so that opposing strands with identical anchorage locations were jacked in pairs to predetermined loads in three stages. Similar to tightening cylinder heads on combustion engines, progressively increasing staged loading provided two benefits: maintained balanced strain and reduced losses in the first strands stressed. Without staging, the first strand was calculated to lose approximately 0.8 kip (4 kN) from the subsequently loaded strands and the associated elastic compression of the concrete.

In theory, the more stages used, the better, because the force difference between the post-tensioning strands is smaller, resulting in more uniform concrete precompression. Conversely, fewer stages are preferred when addressing field efficiency. A practical upper limit to the amount of force increase in a strand that can be attained with subsequent pulls is controlled by the imprints made on the strand by the wedges. If a subsequent strand pull does not cause enough elongation to move a given strand imprint to the next wedge tooth, the wedge will catch and reseat in the original imprint. Therefore, it is desirable to ensure that subsequent strand pulls produce enough elongation to at least exceed the tooth pitch in the wedge (25 teeth/in. [1 tooth/mm]). Balancing these considerations, three stages were used for the first spliced specimen and two stages were used for the second spliced specimen. **Figure A7** shows the stressing in progress.

**Table 1** shows the losses in the first stressed strand from subsequent pulls from the three-stage option. Using the same information from Table 1, all strands essentially end at

**Table 1.** Losses in the first stressed strand from subsequent strands (three-stage option)

Strand loaded	Forces in first strand stressed, kip		
	Stage 1	Stage 2	Stage 3
1	7.00	18.50	26.50
2	6.94	18.45	26.46
3	6.88	18.40	26.43
4	6.82	18.35	26.39
5	6.76	18.30	26.36
6	6.70	18.24	26.32
7	6.64	18.19	26.29
8	6.58	18.14	26.25

Note: 1 kip = 4.448 kN.

different loads, where the last strand stressed ends with 26.5 kip (118 kN) and the first strand stressed ends with 26.25 kip (116.8 kN). This translates into an average strand force of 26.4 kip (117.4 kN) and an effective stress due to post-tensioning of 1077 psi (7426 kPa).

## Second laboratory specimen

A second laboratory specimen was cast to implement the identified improvements in anticipation of full-scale commercial casting operations that involved 24 in. (610 mm), 20-strand systems (**Fig. 1**). The improvements were intended to prevent debris from entering the post-tensioning ducts, prevent epoxy from filling the grouting ducts, and simplify assembly during splicing by extending the length of the strands in the bottom segment from 6 to 8 ft (1.8 to 2.4 m). In addition, the role of deformed ducts in enhancing ultimate capacity was explored. This was achieved by creating indentations around the duct circumference spaced at 2 in. (50 mm) along the length of the ducts, based on pull-out tests performed on deformed ducts after the first trial.<sup>1,4</sup>

The procedures for casting the pile segments and splicing were identical to those used for the first laboratory specimen, except the post-tensioning operation was conducted in two stages, instead of three. **Figures 2, 3, and A8** show the details of these changes. The second-stage target jacking force was 34 kip (150 kN) based on the knowledge from part 1<sup>1</sup> that wedge-setting losses would be approximately 6.5 kip (29 kN).

## Fabrication of full-sized spliced piles at commercial facility

Three 24 in. (610 mm) square piles were cast to demonstrate the scalability of the new post-tensioning pile splice concept and to verify bending capacity. The spliced pile was made from two 20 ft (6 m) long segments, and two controls were each 40 ft (12 m) long. A second control was cast to assess

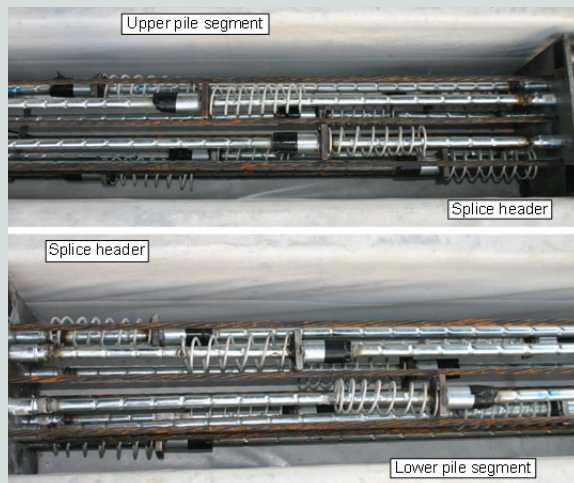


**Figure 2.** Staggered anchorages with deformed ducts bolted to splice header.

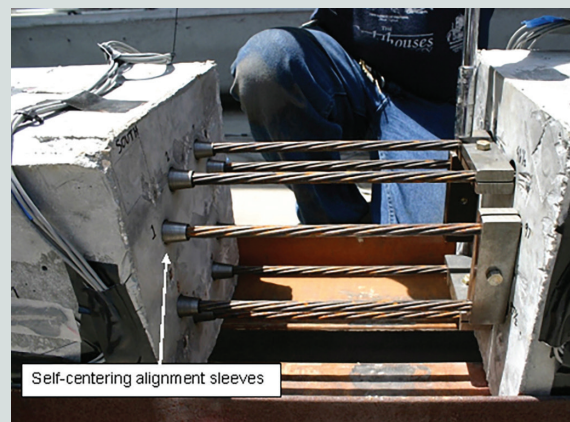


**Figure 3.** Alignment sleeves prevented epoxy from filling duct during final contact. The clamps on the upper segment strands (right) prevented inward slippage and were removed after all strands were inserted in lower segment (left).

the effect of increased spiral spacing near the midpoint, which matched the spacing in the splice region of the spliced pile (Fig. A9).

## Fabrication of components

The 24 in. (610 mm) pile required 20 ducts and a total of 40 anchorage assemblies (Fig. 1). Preparations included fabrication of anchorage assemblies, confinement coils, deformed ducts, and grout manifolds. In addition, a larger 24 in. splice header assembly plate was designed and fabricated (Fig. A10). All plate surfaces in the header were machined to be perfectly flat and parallel.

## Casting full-scale pile specimens

To simplify construction, the internal components of the splicing systems were preassembled as five-duct interchangeable panels, one for each of the four sides of the splicing reinforcing pattern (Fig. A11). The predetermined duct spacing was based on the strand configuration of the fabricator's bed. The first anchor position was set at a distance of one pile diameter from the splice interface (24 in. [610]), and the same 10 in. (250 mm) stagger spacing was retained for the remaining ducts on each side. This five-stagger configuration meant that four of the twenty anchors were the same distance from the splice interface (24, 34, 44, 54, and 64 in. [610, 860, 1120, 1370, and 1630 mm]) and each segment used interchangeable panels. While the upper and lower pile segments used four of these panels, the upper pile panels were equipped with shims that restrict wedge movement, as discussed in part 1.<sup>1</sup> Duct extensions were installed separately in the upper pile segment from the interchangeable panels to the top of the pile where post-tensioning forces would be applied.

Casting of the splice pile segments followed standard procedures: the splice header was inserted in the bed as a normal pile separation header, and strands were progressively threaded through the headers in order from bottom to top before the ducts were installed and spiral reinforcement was pulled.

The duct assemblies and all long lengths of duct extensions were placed in the bed after the strands were tensioned but before the spirals were pulled to the ends of the pile. Two top strands were left slack to ease installation and were tensioned only after all splicing fixtures were installed. Figure 4 shows the finished bed.

## Splicing full-scale pile specimens

The cured pile specimens were transported to a different location for splicing and flexural testing.

## Preparations for splicing

In preparation for splicing, a borescope was used to inspect all ducts for debris and check the spring movement of embedded wedges. With the two pile segments sufficiently separated, twenty individual splicing strands (approximately 33 ft [10 m]) were fed into the upper pile segment, with exposed strands clamped to ensure no upward slippage while inserting the strands in the lower pile segment (Fig. 5). A length of 10 ft (3 m) was left at the base of the upper pile segment, and a length of 3 ft (0.9 m) was exposed out of the top of the upper pile segment. Alignment sleeves were installed after all strands were in place. The lower exposed strand lengths were staggered in 1 in. (25 mm) increments so only one strand at a time would come into contact with the lower pile segment. The flexibility of the long (10 ft) exposed lengths aided in manipulating and inserting strands into the lower segment.

Like the 14 in. (360 mm) splice piles, the 24 in. (610 mm) pile

specimen was spliced horizontally and nonsag epoxy sealant was applied to the splicing surfaces before bringing the piles in close contact. The upper pile segment was placed on rollers, and a forklift was again used to push the two segments together with the lower segment remaining fixed. Strand clamps (not shown) were removed once the two pile segments were in close proximity.

### Post-tensioning splicing

The post-tensioning stressing order was determined as before so that each pair of opposite strands was jacked to predetermined loads and balanced strain was maintained. Three load steps were used to reduce losses from elastic shortening of the concrete. The stressing order of matched pairs was marked on the jacking header plate for convenience. Strands 1, 2, 3, and 4 were all anchored at the same locations and so on in groups of four corresponding to similarly positioned anchorages on all four faces of the pile.

**Figure A12** shows the computed stresses based on strain gauge measurements on either side of the splice. At the conclusion of the splicing process, the final stress distribution reflected the linear distribution created by staggering the anchorages.<sup>1</sup> The stress induced at the splice was slightly less than the target 1000 psi (7000 kPa) value. The post-tensioned strand ducts were then grouted (**Fig. A13**).

### Flexural testing of spliced and control specimens

Two series of ultimate flexural tests were conducted, one for specimens cast in the laboratory and the other for the specimens cast at a commercial prestressing facility. The intent of all of the tests was to establish the extent to which spliced

piles met FDOT performance standards.<sup>3</sup> The test setup was based on procedures used by FDOT to evaluate spliced piles.<sup>5,6</sup>

### Laboratory testing

Two spliced piles and their respective controls were tested over a two-day period both 56 and 90 days after they were cast. The measured compressive strength at the time of testing was 9104 psi (62.77 MPa) at 56 days and 9377 psi (64.65 MPa) at 90 days.

**Figure 6** shows the four-point bending configuration where the 20 ft (6 m) long, 14 in. (360 mm) piles were tested on a 19 ft (5.8 m) span. Two equal point loads were applied to provide a 4 ft (1.2 m) constant moment zone. However, when considering the additional load from self-weight, the maximum moment was at midspan.

Load cells measured the applied loading; deflections at the middle and quarter points were measured using linear variable differential transformers. Surface bonded strain gauges were used to monitor concrete strain in compression and tension over the bending depth of the pile. **Figure 7** shows the failure modes for the control and spliced piles.

The observed failure mode of the control piles was tension-controlled in which the compression concrete crushed after the prestressing steel yielded. The compression block extended below the top strands and the spirals. Both control piles exhibited multiple tension cracks and large permanent deformations. The failure loads for control piles 1 and 2 were 39.2 kip (174 kN) and 39.4 kip (175 kN), respectively.

Failure in the spliced piles (**Fig. 7**) initiated in the compress-



**Figure 4.** Fully stressed bed with lifting hooks (left) and splicing header connection (right).

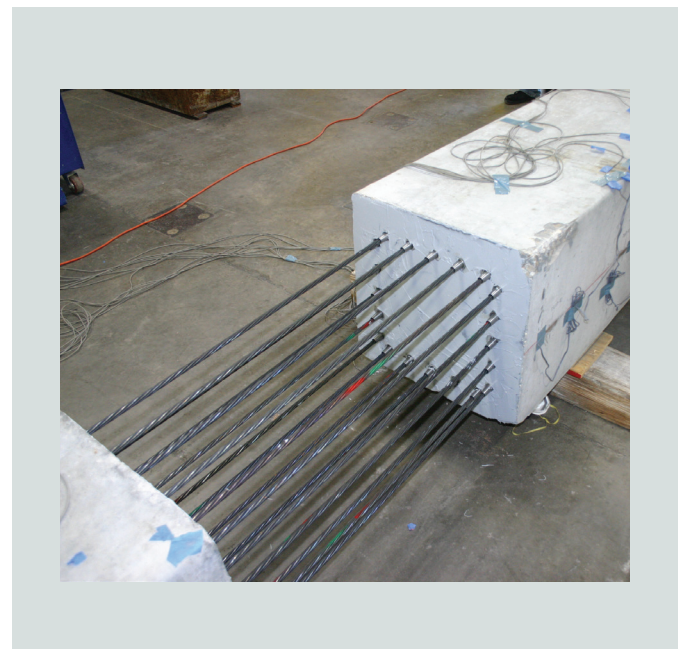


**Figure 5.** All strands passed the lower pile wedges.

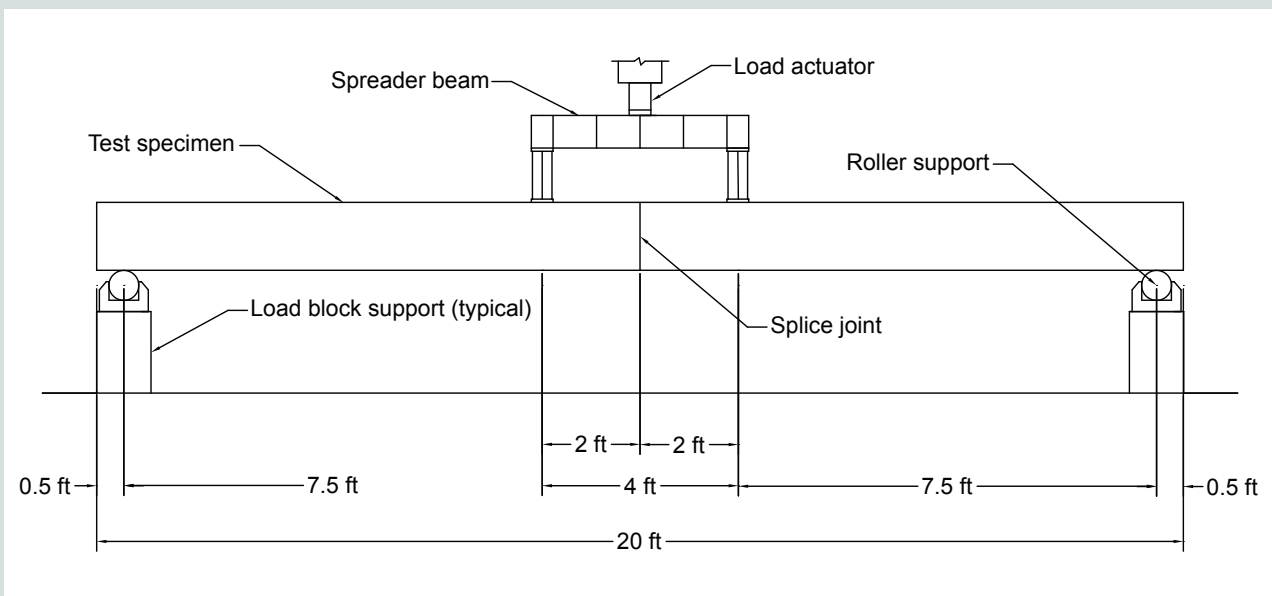
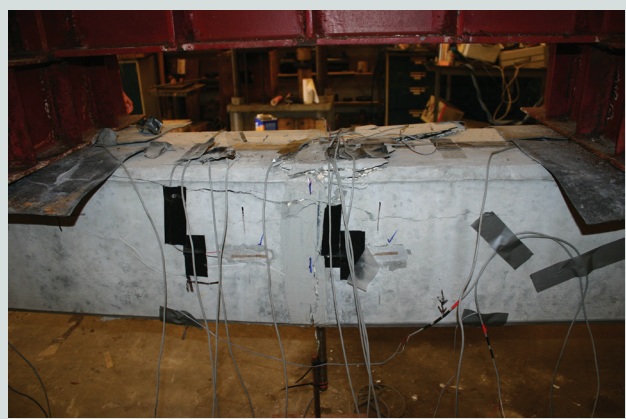


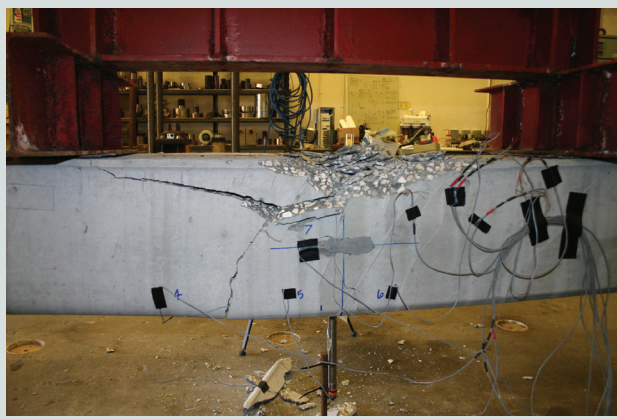
**Figure 6.** Test setup for laboratory specimens. Note: 1 ft = 0.305 m.



Control pile 1



Splice pile 1



Control pile 2



Splice pile 2

**Figure 7.** Failure modes.



**Table 2.** Comparison of cracking and failure loads

Event	Test 1			Test 2		
	Splice	Control	Ratio	Splice	Control	Ratio
Cracking load, kip	14.6	16.5	0.88	15.0	16.8	0.89
Failure load, kip	32.8	39.2	0.84	36.0	39.4	0.91

Note: 1 kip = 4.448 kN.

sion region after there was separation along the splice joint in the tensile region. While the control piles exhibited multiple cracks distributed throughout the constant moment region, the spliced specimens only developed one crack at the splice interface. The absence of other cracks in the constant moment zone was to be expected because the tensile resistance in the spliced pile was greater adjacent to the splice, due to the additional cracking resistance from the native prestressing strands. As a result, compression failure was focused on a smaller area above the spiral depth in the cover. Spliced pile 1 rebounded almost fully and had a failure load of 32.8 kip (146 kN). Spliced pile 2 had a failure load of 36 kip (160 kN). Loading continued past failure, which led to debonding of the compression block without any additional gain in load and which

resulted in a larger permanent deformation than splice pile 1.

Both spliced piles rebounded far more than the controls due to less distortion from a single crack and a smaller compression failure zone. The deformed ducts led to load transfer from the splicing strands to the native prestressing strands, which accounted for higher flexural stiffness of the second spliced pile.

### Observations from laboratory specimen test results

**Table 2** compares the cracking and ultimate loads of the spliced piles with their respective controls. The ratio column is the splice/control value. Both ultimate and cracking values were

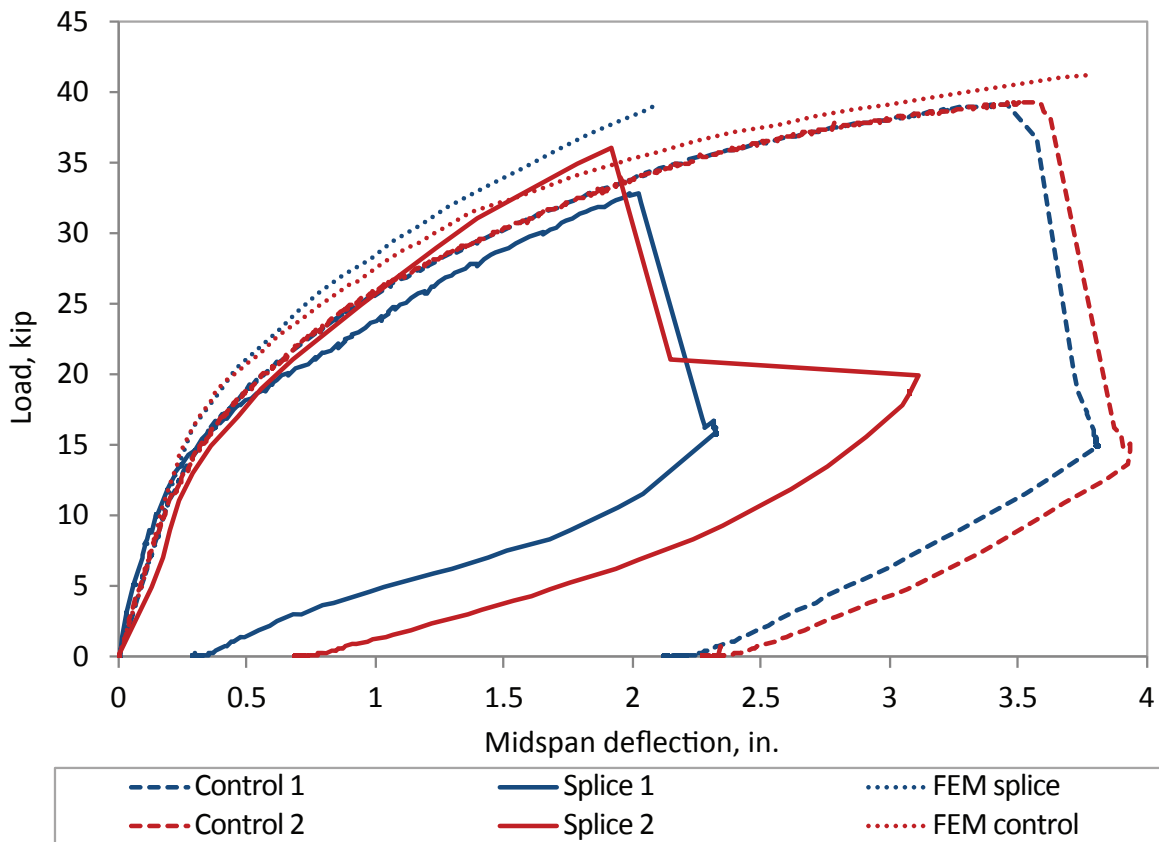


**Figure 8.** Midspan deflection versus load for control and spliced piles. Note: FEM = finite element model. 1 in. = 25.4 mm; 1 kip = 4.448 kN.

smaller for the spliced piles. Ultimate capacities ranged from 84% (smooth ducts) to 91% (deformed ducts) of the control capacity. The corresponding cracking loads were 88% to 89%.

The smaller ultimate capacity was anticipated because there were fewer post-tensioning strands at the extreme layer (two, compared with three in the controls in Fig. 1). The lower crack load indicated that the post-tensioning stress was not as high as that from prestress due to the losses in the short post-tensioning strands. As expected, cracking was not observed in the epoxy but rather in the adjacent concrete.

### Finite element analysis

Finite element analysis was conducted to better understand how the structural response of the spliced pile differed from that of the unspliced control. Three-dimensional models were developed for the entire pile (both sizes). Modeling used elements available in the finite element software library: concrete was idealized using block elements capable of cracking in tension and crushing in compression, prestressing strands used uniaxial tension-compression elements, and the bearing plates used eight-node elements that have plasticity capabilities. The interface between the two segments in the spliced pile was modeled using contact elements.

The material properties of the interface were based on the tensile bond and elastic modulus of the epoxy as specified by the manufacturer.<sup>4</sup> The grouted splicing strands were assumed to be perfectly bonded to the concrete, and their variable anchorage locations were modeled per the as-built condition. The initial strain method was used to simulate force transfer

to the concrete due to prestressing.<sup>11</sup> Complete details of the modeling may be found elsewhere.<sup>12</sup>

### Comparisons

The validity of the finite element model was established by comparing the predictions with experimental data. **Figure 8** compares the predicted and experimental loads with the mid-span deflection plots from test series 1 (using smooth ducts) and test series 2 (using deformed ducts). The finite element model captured the overall structural response of the control and spliced piles. Agreement is better for test series 2 using deformed ducts because of the assumption of perfect bond.

Up to the point of cracking, both the control and splice piles exhibited similar longitudinal strain distributions. However, after cracking and given that the splice pile cracking was isolated to the splice region, the two exhibited different strains throughout. This was apparent along the upper surface in compression where the hinging action of the splice concentrated stress to a smaller region. Loads previously carried across the splice were transferred to the pile through the deformations in the ducts.

The model showed that the stress distribution in the spliced pile (**Fig. 9**) indicated that the concrete in the cover above the splice was crushed. Because this zone is smaller compared with that of the control, the ultimate capacity of the spliced pile was controlled by localized concrete failure. This was confirmed by evaluating the compression strain distribution, where only a small portion of the constant moment region experienced the full failure strain (**Fig. 9**). Although the center

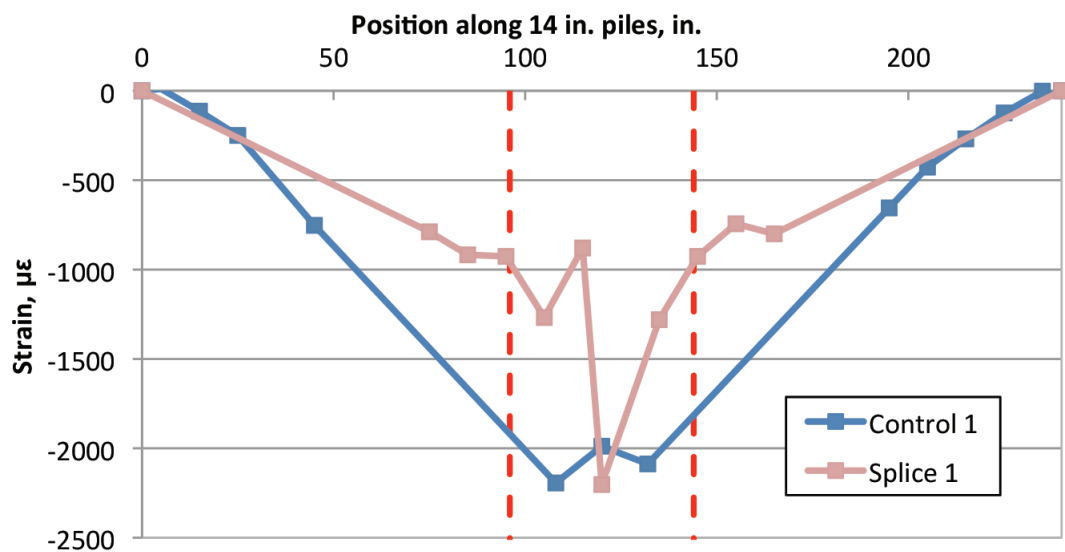
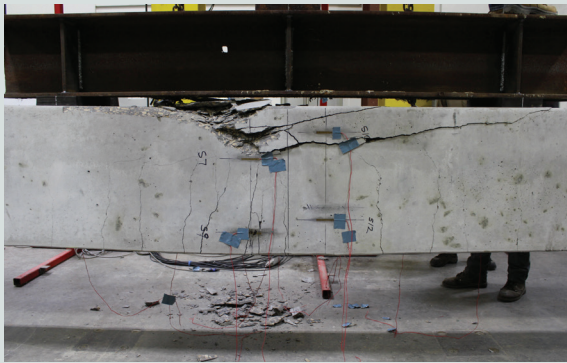
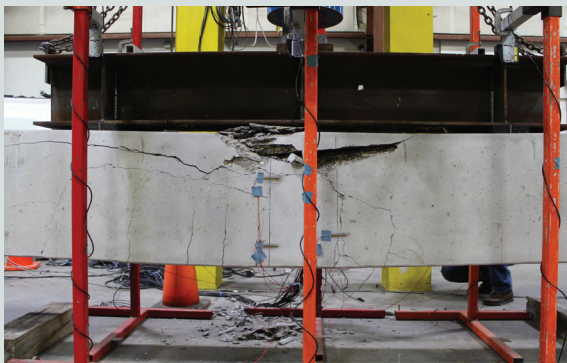


**Figure 9.** Measured compression strain distribution in 14 in. piles at failure. Note: 1 ft = 0.305 m.



Control C-1 (tight spiral layout)



Control C-2 (standard)

**Figure 10.** Failure modes in full-scale controls.



**Figure 11.** Failure mode in full-scale spliced pile.

**Table 3.** Comparison of cracking and failure loads

Event	Splice	Control			
		Standard	Ratio	Tight	Ratio
Cracking, kip	38.7	39.6	0.98	40.2	0.96
Ultimate, kip	80.8	84.8	0.95	85.4	0.95

Note: 1 kip = 4.448 kN.

of the pile length was a constant moment region, it was not a constant stress region due to the changing cross-sectional properties across the splice region.

## Full-scale testing

One spliced pile and two controls were tested in flexure. One of the two controls (C-1) had a tight spiral layout spaced in an identical manner (Fig. A9) to the spliced pile at midspan. The other (C-2) had the standard spiral layout. The tests were conducted on two consecutive days, 65 and 66 days after casting. The measured concrete strength was 12,193 psi (84.071 MPa).

The four-point bending configuration was similar to that shown in Fig. 6 with the exception that the overall span was 38 ft and the two equal point loads were applied 6.5 ft (2 m) apart to create the constant moment zone. The maximum moment under combined dead and applied load was again at the midspan of the splice.

**Figures 10 and 11** show the failure modes of the controls and the spliced pile, respectively.

## Observations from full-scale test results

**Table 3** compares the cracking and ultimate loads of the spliced pile with the two one-piece controls. The ultimate capacity of the spliced pile was 95% of the control; the cracking moment was between 96% and 98%. These were higher than those for the laboratory specimens (Table 2). The larger effective depth (21 in. [530 mm], compared with 11 in. [280 mm] for the laboratory specimens) meant that the contribution of the ultimate moment was not just from the post-tensioning strands located at the extreme lower level but also from more strand levels below the neutral axis. The effectiveness of the lowest strands was also improved compared with the laboratory specimens where the splice-to-native strand ratio increased from 2/3 to 5/6 (Fig. 1).

The overall responses of the laboratory and full-scale specimens were similar. In controls, multiple tension cracks formed in the constant moment zone. In the spliced pile, tension cracking was initiated at the spliced joint, which opened as the load was increased further. Concentrating the distortion to a single crack again showed that the compression stress was focused on a smaller zone. **Figure 12** shows the strain along the upper face in the constant moment region of the 24 in. (610 mm) piles. The highest strains were closest to the splice, while the one-piece controls maintained a relatively uniform strain throughout the constant moment region. All piles failed at the same approximate peak compression strain.

## Finite element analysis

Based on procedures discussed earlier, the 24 in. (610 mm) piles were also modeled using the same finite element approach. **Figure 13** shows comparisons of the predicted and observed loads with the midspan deflection plots from all

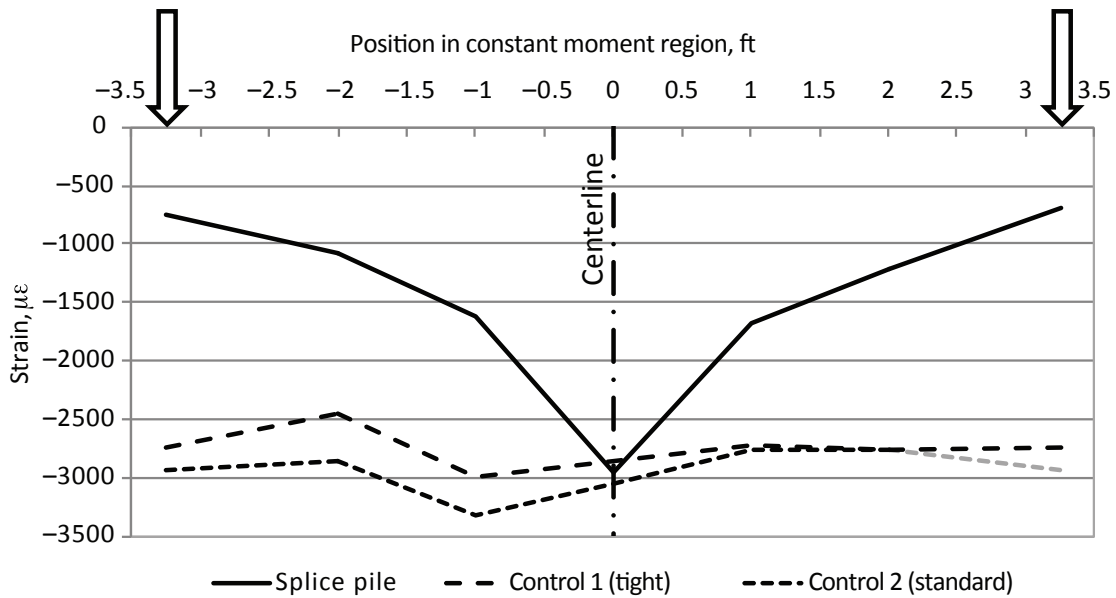


**Figure 12.** Compression strain along upper face in the constant moment region of the 24 in. (610 mm) piles. Note: 1 ft = 0.305 m.

tests. Again, the predictions from the finite element models captured the overall structural response of the test specimens where the splice pile response was stiffer.

**Figure A14** shows the modeled longitudinal stress distribution at midspan (constant moment) for the control and spliced

piles at ultimate. Similar to the smaller piles, the compression failure region in the spliced pile was much smaller than that in the control pile, as was observed in the testing (Fig. 10 and 11). The analysis suggests that tensile separation at the splice interface bottom acted as a larger pivot about which the section rotated, compared with the much shallower laboratory speci-

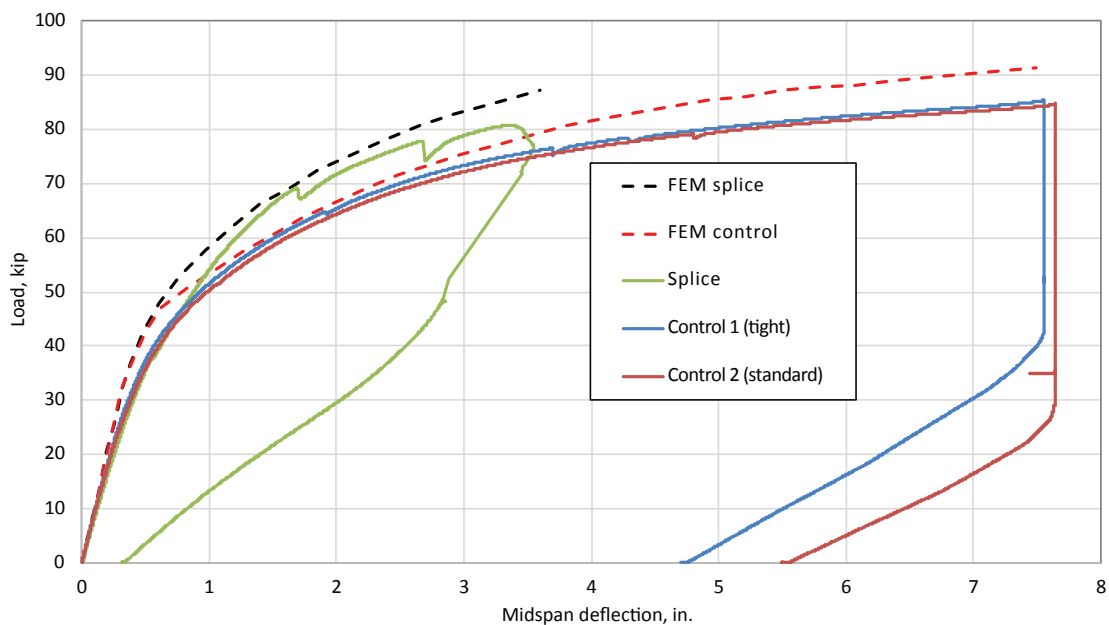


**Figure 13.** Midspan deflection versus load for the control and spliced piles. Note: FEM = finite element model. 1 in. = 25.4 mm; 1 kip = 4.448 kN.

mens (Fig. 7). As a result, the compression failure zone in the spliced pile was limited to an even smaller region compared with the laboratory specimens. Modeling again confirmed that the constant moment region did not produce constant stress.

During testing (Fig. 11), tensile cracking initiated at the splice and progressed diagonally within the concrete. Based on the finite element model, the principal stress vector fields became inclined in the vicinity of the joint, indicating the possibility of diagonal cracks. **Figure A15** shows the experimental and predicted cracking patterns at the splice joint.

## Discussion

The goal of this research project was to develop a spliced pile that could withstand loads comparable to one-piece, unspliced piles.<sup>3</sup> The results demonstrated conclusively the scalability of the new post-tensioning method and its ability to meet and exceed performance standards. The spliced pile (744.6 kip-ft [1009 kN-m]) exceeded the FDOT required moment capacity for a 24 in. (610 mm) prestressed concrete pile (600 kip-ft [814 kN-m]), **Table 4**.

The critical moments imposed on a pile section are caused by extreme events, such as ship impact, and occur directly below the pile cap. In some cases, prestressed concrete piles are cast with large reinforcing bars in this region of the pile to bolster moment capacity.<sup>13</sup> A byproduct of the new pile splice system is the presence of the continuing unstressed strand in the upper segment that coincides with the region of higher moments. A 21% increase in moment capacity (941 kip-ft [1276 kN-m], **Table 4**) was shown in a separate bending test of just the upper spliced pile segment.<sup>4</sup>

The core elements of the conceptual design, such as staggered anchorages, confinement coils, and dually embedded anchorages, did not change throughout the laboratory to full-scale transition.<sup>1</sup> The only change that improved performance was the use of deformed ducts. Most changes were to simplify fabrication, for example, the use of panels, sealing the openings of the ducts, the locations of grouting manifolds, and increasing the lengths of the strands beyond the embedded anchorages.

**Table 4.** Bending strengths of 24 in. (610 mm) piles

Pile	Bending strength, kip-ft
C-1	780.8
C-2	776.1
Splice interface	744.6
FDOT requirement	600.0
Upper segment	941.4

Note: FDOT = Florida Department of Transportation. 1 kip-ft = 1.356 kN-m.

Additional improvements in constructibility were made in the fabrication of the full-sized piles that were driven and presented in part 2.<sup>2</sup> Therein, the shape of the anchorage plates was sculpted to optimize the available bearing area around the ducts and to reduce congestion with neighboring strands and ducts.

The piles tested were spliced in the horizontal position due to laboratory restrictions. The splice would normally be completed in a vertical position, which minimizes bending stresses during post-tensioning induced by self-weight. Vertical splicing can be done in the following ways, depending on contractor scheduling:

- splice, drive immediately, and grout later
- splice, grout, and drive with wet grout
- splice, grout, wait, and drive fully cured

No adverse effects are foreseen in driving with uncured epoxy or liquid grout. The third option was tested and is presented in part 2.<sup>2</sup> Contractors, therefore, have flexibility to adapt to construction schedules. A change in the alignment dowel design allowed the ducts to fully seal and withstand high-pressure grouting operations, even when the epoxy was not cured.<sup>2</sup>

Unplanned splices have the potential to use the same upper pile design as presented, but provisions for drilling the bottom pile would still be needed. This also requires the strands to be bonded in the lower pile. High early strength grouts have shown great potential in fitting this scenario in a timely fashion. Grouting the splice strand ducts would follow in the same manner described herein.

## Lessons learned

Each splice pile tested provided usable feedback to further the advancement of the overall splice concept. For the 24 in. (610 mm) pile tests, the following lessons were learned:

- Concreting the splice pile can be made easier by reducing the number of splicing strands, thereby using the next-larger-sized strand (for example, sixteen 0.6 in. [15 mm] diameter splice strands instead of twenty ½ in. [13 mm] diameter special strands). This can also reduce splicing time. However, it is more cost-effective and efficient only if the reduced number of strands is divisible by four, to maintain balanced post-tensioning stresses and bending capacity in all directions.
- The washer insert used to reduce wedge set losses may restrict strand pass-through if the quarter-turn spring cap on the chuck is inadvertently left in the compressed state in the casting bed. Threaded-screw-cap chucks with no spring backlash should be used to fully control final in-bed tolerances (avoid quarter-turn back caps). This complication manifested in difficult strand installation when preparing the upper pile segment before splicing.

- Grouting was successful but slow due to restrictions in and around the wedges. Grout was pumped through the ducts and passed through the three slits that formed around the three wedges. Enhanced passageways should be considered to speed the grouting process, or a less viscous grout could be considered.
- The high pressure used to pump grout through the wedges also forced some grout to find alternative pathways out of the pile in the splice region because grouting was performed before the epoxy cured. No adverse effects were noted as a result of the grout paths through the epoxy at the time of bending tests. However, an alternate alignment coupler design was shown to eliminate grout leakage, allowing the contractor the option to grout immediately while the epoxy is uncured.<sup>2</sup>

## Conclusion

This paper provides an outline of a research and development effort to demonstrate the merits of a new splicing system for prestressed concrete piles. The developed post-tensioning system addressed stress concentration, corrosion prevention, and anchorages that can be problematic. In this study, the problem of stress concentration at the anchorages was solved by staggering and using confinement coils to increase localized concrete strength. Prestressing chucks were incorporated into anchorages welded to steel ducts. Shims were deployed to reduce anchor set losses. The anchorages were embedded and, therefore, protected from corrosion. The scalability of the design concept was demonstrated by the fabrication of a full-scale 24 in. (610 mm) pile at a commercial prestressing facility. In fact, larger piles were shown to be less affected by the reconfigured splicing strand layout relative to the native pile strands.

The experimental results of the laboratory and full-scale specimens demonstrated that the spliced piles met and exceeded the performance requirements specified by FDOT, which are similar to those in most states. The spliced pile separated at the splice, and no other cracks developed in the constant moment zone. When extreme event loads occur, the structure will rebound to near the original position.

The findings of this study suggest that the new splice design can effectively develop full capacity for the purposes of withstanding pile driving and structural loading. Therein, full prestress levels were transferred through the splice zone, which no other commercial method provides. In addition, the splice design provides full corrosion protection because no components of the splice breach the concrete cover.

## Acknowledgments

This study was funded by a grant from FDOT. The opinions, findings, and conclusions expressed in this publication are those of the authors and not necessarily those of FDOT or the U.S. Department of Transportation. The authors would like to further thank CDS Manufacturing Inc. for its willingness to participate in the study.

## References

1. Mullins, G., K. Johnson, and R. Sen. 2018. "Post-tensioned Splice System for Precast, Prestressed Concrete Piles: Part 1, Conceptual Design." *PCI Journal* 63 (1): 26–39.
2. Mullins, G., Z. Wu, K. Johnson, and R. Sen. 2018. "Post-tensioned Splice System for Precast, Prestressed Concrete Piles: Part 2, Field Implementation and Driving Spliced Pile." *PCI Journal* 63 (3): 28–40.
3. FDOT (Florida Department of Transportation). 2016. *Standard Specifications for Road and Bridge Construction*. Tallahassee, FL: FDOT.
4. Mullins, G., and R. Sen. 2015. "Investigation and Development of an Effective, Economical, and Efficient Concrete Pile Splice." Final research report. Tallahassee, FL: FDOT.
5. Ansley, M. 2002. *Load Test on Sure-Lock Square Pile Splice*. Tallahassee, FL: FDOT.
6. Beitelman, T. 2011. *Structural Performance of ICP PHC Piles*. Tallahassee, FL: FDOT.
7. FDOT. 2016. *Design Standards for Design Construction, Maintenance and Utility Operation on the State Highway System, Indices 20614 and 20624*. Tallahassee, FL: FDOT.
8. ACI (American Concrete Institute) Committee 503. 2002. *Guide for the Selection of Polymer Adhesives with Concrete (Reapproved 2003)*. ACI 503.5R-92. Farmington Hills, MI: ACI.
9. Naaman, A. E. 2012. *Prestressed Concrete Analysis and Design*. 3rd ed. Ann Arbor, MI: Techno Press 3000.
10. Cook, R., M. McVay, and K. Britt. 2003. *Alternatives for Precast Pile Splices – Parts 1 and 2*. Final report to FDOT, report BC354 RPWO #80. Gainesville, FL: University of Florida Department of Civil and Coastal Engineering.

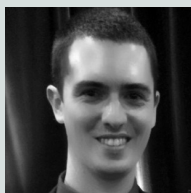
11. Kang, Y. 1977. "Non-linear Geometric, Material, and Time Dependent Analysis of Reinforced and Prestressed Concrete Frame." PhD diss., University of California, Berkeley, CA.
12. Wu, Z. 2016. "Flexural Behavior of Post-Tensioning Spliced Prestressed Concrete Piles." PhD diss., University of South Florida, Tampa, FL.
13. Mullins, G. 2014. Direct conversation with Charles Rudie, Parsons Brinkerhoff Inc., design engineer for the Choctawhatchee Bay Bridge, FL, March 19.

## About the authors



Zhongxin Wu, PhD, PE, is an associate professor in the Department of Civil Engineering at the Shenyang City University in China. He received his MS and PhD in civil engineering from the University of South Florida (USF) in Tampa. He has worked as a

senior structural engineer in the United States since 2000. He was responsible for the analysis and design of bridges, seaports, and cruise terminals, including steel and reinforced, prestressed, and post-tensioned concrete projects. He received the 1997 USF Graduate Fellowship and 2003 CH2M Hill Engineering Project Award.



Kevin Johnson, PhD, is a senior engineer with Earth Tech in Land O' Lakes, Fla. He received his BS, MS, and PhD from USF with concentrations in structural and geotechnical design. His research focused on the design and construction of deep foundations,

including thermal integrity analysis of drilled shafts, post-tensioned splices for prestressed concrete piles, and evaluation of mineral and polymer slurries for drilled shafts. He received the International Association of Foundation Drilling Industry Advancement Award in 2012 and the Deep Foundations Institute Outstanding Paper Award in 2015.



Gray Mullins, PhD, PE, is a professor in the Department of Civil and Environmental Engineering at USF, where he also received his BS, MS, and PhD. He received the 2015 Charles Pankow Award, 2014 Ben Gerwick Award, 2013 C. William

Birmingham Innovation Award, and 2013 Nova Award for innovation in foundation design, construction, and quality assurance. He has received eight patents reflecting innovations in these areas.



Rajan Sen, PhD, PE, is a professor of civil engineering at USF, where he held the inaugural Samuel and Julia Flom Endowed Chair and joint appointments in the College of Engineering and School of Architecture and Community Design. An alumnus

of the Indian Institute of Technology Kharagpur, he holds graduate degrees from the University of British Columbia in Vancouver, BC, Canada, and the University at Buffalo, The State University of New York, and has worked for a decade at the Highway Engineering Computer Branch and Bridges Engineering Standards Division at the Department for Transport in London, U.K. A Fellow of the American Concrete Institute and the American Society of Civil Engineers, he is a Jefferson Science Fellow and served as senior advisor at the U.S. Department of State in Washington, D.C.



## Abstract

Splicing precast, prestressed concrete piles has historically been difficult because the attachment detail requires either preplanned considerations and cast-in connection details or onsite coring and doweling when unplanned pile extensions are needed. When the piles are driven after splicing, the splice connection is prone to tensile failures due to the inability to transfer tensile driving stresses through the connection and into the other pile segment. Focusing on preplanned splices, the Florida Department of Transportation limits tension stresses during driving to 250 and 500 psi (1700 and 3400 kPa) for epoxy dowel splices and mechanical splices, respectively. This can limit the ability to efficiently drive the pile to the point that it may even be impossible. In response to the need for a more robust splicing methodology, an alternative pile-splicing approach incorporating post-tensioning was developed. The concept eliminates the limitations on tension stresses during driving. This is the third of three papers that details the development and implementation of the new approach into a prototype system. This involved laboratory and full-scale studies and subsequent ultimate load verification tests. The findings show that the concept is scalable and implementable in commercial facilities with minor adjustments.

## Keywords

Cast-in connection details, connection, coring, doweling, load, pile extension, splice connection, splicing.

## Review policy

This paper was reviewed in accordance with the Precast/Prestressed Concrete Institute's peer-review process.

## Reader comments

Please address any reader comments to *PCI Journal* editor-in-chief Emily Lorenz at [elorenz@pci.org](mailto:elorenz@pci.org) or Precast/Prestressed Concrete Institute, c/o *PCI Journal*, 200 W. Adams St., Suite 2100, Chicago, IL 60606.